Study of light sterile neutrino at the long-baseline experiment options at KM3NeT

Dinesh Kumar Singha,[1,*] Monojit Ghosh,[1,2,†] Rudra Majhi,[1,‡] and Rukmani Mohanta[1,§]

[1]*School of Physics, University of Hyderabad, Hyderabad 500046, India*
[2]*Center of Excellence for Advanced Materials and Sensing Devices, Ruder Bošković Institute, 10000 Zagreb, Croatia*

(Received 10 November 2022; accepted 4 April 2023; published 28 April 2023)

In this paper, we study the capability of different long-baseline experiment options at the KM3NeT facility, i.e., P2O, upgraded P2O, and P2SO to probe the light sterile neutrino and compare their sensitivities with DUNE. The P2O option will have neutrinos from a 90 KW beam at Protvino to be detected at the ORCA detector, the upgraded P2O will have neutrinos from the upgraded 450 KW beam to be detected at the ORCA detector and the option P2SO will have neutrinos from a 450 KW beam to be detected at the upgraded Super-ORCA detector. All these options will have a baseline around 2595 km. Our results show that the experiments at the KM3NeT (DUNE) would be more sensitive if the value of Δm^2_{41} is around 10 (1) eV^2. Our results also show that the role of near detector is very important for the study of sterile neutrinos and addition of near detector improves the sensitivity as compared to only the far detector for the $3+1$ scenario. Among the three options at KM3NeT, the sensitivity of P2O and upgraded P2O is limited and sensitivity of P2SO is either comparable or better than DUNE.

DOI: 10.1103/PhysRevD.107.075039

I. INTRODUCTION

The phenomenon of neutrino oscillation has been well established by a variety of experiments like solar, atmospheric, reactor, accelerator etc. As a consequence of neutrino oscillation, neutrinos have to be massive possessing nonzero but small masses. Now we have entered the era of precision measurement of neutrino oscillation parameters along with the determination of the remaining unknowns in standard three flavor scenario [1]. Neutrino experiments thus provide an window to explore physics beyond the standard three flavor scenario. There are several such formulations exist in the literature, whose signatures can be probed through neutrino oscillation experiments. The possibility of having more than three neutrinos in nature has been discussed for a very long time among the physics community. If there exists a fourth neutrino, then it has to be sterile which can mix with the other three active neutrinos. Several experimental anomalies also hint toward the existence of an extra sterile neutrino [2]. Some crucial anomalies being the backbone of sterile neutrinos are LSND [3] anomaly where a significant excess events have been seen over the known backgrounds, MiniBooNE [4] low energy excess while charged pion decay during flights, reactor [5] and Gallium [6] anomalies associated with an overall normalization discrepancy of electron antineutrinos. The recent results of MicroBooNE [7] have sparked the discussion of the light sterile neutrinos once again. According to MicroBooNE, there is no excess of ν_e events coming from the ν_μ beam. However, Ref. [8] studies the same set of MicroBooNE data and shows that an analysis with the electron disappearance channel is consistent with oscillations governed by sterile neutrinos. In reply to that, MicroBooNE performed a joined fit taking the ν_e appearance and ν_e disappearance channel and show that three neutrino fit still gives a better fit than four neutrino fit at 1σ [9]. In addition, a combined fit of MiniBooNE and MicroBooNE shows that the $3+1$ model is still allowed at a significant confidence level [10]. Apart from these accelerator results, the gallium-based experiment BEST [11] and reactor based experiment Neutrino-4 [12] recently reported a positive signal for a light sterile neutrino. On the other hand, the atmospheric data from the IceCube experiment is consistent with the no sterile neutrino hypothesis [13]. From the above discussions, we understand that the situation with a light sterile neutrino is still very intriguing and we need future data for arriving at a conclusive decision.

*dinesh.sin.187@gmail.com
†mghosh@irb.hr
‡rudra.majhi95@gmail.com
§rmsp@uohyd.ac.in

In this paper, we would like to study the sensitivity to the light sterile neutrinos at the long-baseline options of the KM3NeT facility [14]. The original aim of this facility is to detect the astrophysical neutrinos but recently there are discussions to send a neutrino beam from the accelerator in Protvino, Russia and detect these neutrinos at the detector at the KM3NeT facility [15]. In this case, the distance from the source to the detector will be around 2595 km and energy of the neutrinos will be a few GeV. At this moment, three options of this experiment are under consideration: (i) neutrinos arising from a 90 KW proton beam from the accelerator at Protvino to be detected at the ORCA detector at the KM3NeT facility. We call this configuration as P2O, (ii) neutrinos generating from an upgraded 450 KW beam to be detected at ORCA detector. We call this configuration as upgraded P2O and (iii) neutrino arising from an updated 450 KW beam to be detected at the updated Super-ORCA detector. We call this configuration as P2SO. The upgraded 450 KW beam as compared to 90 KW beam will produce a more intense beam of the neutrinos whereas an updated Super-ORCA detector over the ORCA detector will provide better efficiency to accept signal events and reject background events. In this work, we will consider all the three configurations as mentioned earlier to estimate the sensitivity of these experiments to a light sterile neutrino and compare their sensitivity with another upcoming long-baseline experiment DUNE [16]. In our work, we consider two scenarios: (i) assuming the light sterile neutrino does not exist in nature, we will estimate the upper bound on the sterile mixing parameters and (ii) assuming that a light sterile neutrino exists in nature, we will estimate how the sensitivity of these experiments to measure the current unknowns in standard three flavor scenario is getting affected. We consider both far and near detectors in our analysis. To the best of our knowledge, this is the first work estimating the sensitivity to sterile neutrinos at the long-baseline options at the KM3NeT facility. For previous studies regarding the study of light sterile neutrinos in the context of long-baseline experiments, we refer to Refs. [17–36].

The paper is organized as follows. In the next section we discuss the $3+1$ scenario, i.e., how the oscillation in the standard three flavor is altered by the existence of one light sterile neutrino. In Sec. III, we will discuss the configuration of the different experimental setups that we consider in our study. We will also briefly outline the statistical procedure which we adopt to estimate the sensitivity. In Sec. IV, we discuss the sensitivities of different experiments to the sterile neutrinos at the probability level. In Sec. V, we estimate the bound on the sterile mixing parameters assuming there is no sterile neutrino in nature. After that, in Secs. VI–IX, we will study the sensitivity of these experiments to measure the current unknowns in the standard three flavor scenario assuming there exists a light sterile neutrino in nature. Finally, in Sec. X, we summarize our results and then conclude.

II. FORMALISM

In the presence of a light sterile neutrino, the Pontecorvo–Maki–Nakagawa–Sakata mixing matrix U which relates the neutrino flavor states to the mass states, is written in the following way:

$$U = U_{34}(\theta_{34},\delta_{34})U_{24}(\theta_{24},\delta_{24})U_{14}(\theta_{14},0)U^{3\nu}, \quad (1)$$

$$\text{with} \quad U^{3\nu} = U_{23}(\theta_{23},0)U_{13}(\theta_{13},\delta_{\rm CP})U_{12}(\theta_{12},0), \quad (2)$$

where $U_{ij}(\theta_{ij},\delta_{ij})$ denotes a rotation in the (i,j)-plane with mixing angle θ_{ij} and phase δ_{ij}.[1] Neutrino oscillation in the standard three flavor is governed by three mixing angles: θ_{13}, θ_{12}, and θ_{23}, two mass squared differences: $\Delta m^2_{21} = m^2_2 - m^2_1$ and $\Delta m^2_{31} = m^2_3 - m^2_1$, and one phase δ_{CP}. Among these parameters, the current unknowns are: (i) hierarchy of the neutrino masses, (ii) octant of θ_{23} and (iii) the CP violating phase $\delta_{\rm CP}$. In the presence of a sterile neutrino, this mixing scheme is extended by three new mixing angles: θ_{14}, θ_{24}, and θ_{34}, two additional phases: δ_{24} and δ_{34}, and one more mass squared difference: Δm^2_{41}.

At this point, let us briefly discuss our choice of the parametrization of U in $3+1$ scenario. Note that in Eq. (1), the phases can be associated with any of the three mixing angles. For study in short-baseline experiments where the oscillations are mainly governed by Δm^2_{41}, it would be sufficient to associate all the three phases in $U^{3\nu}$ and therefore, in the probability expressions there will be no phases [35]. As we are interested in the long-baseline regime, the phases become important. In case of oscillations governed by Δm^2_{31} only, the ideal way is to put the two phase with θ_{12} and, θ_{13} and to put the other phase with any of the sterile angles [35]. For the $\nu_\mu \to \nu_e$ oscillations at the long-baseline, the oscillations are governed by both Δm^2_{21} and Δm^2_{31}. Therefore, in this case, it is important to associate the sterile phases with the sterile angles [36]. However, the mixing angle θ_{34} appears in the oscillation probabilities only when one considers strong matter effect and neutral current events in the calculation, which we will see in the next paragraph. Therefore, keeping one phase with θ_{34}, one can easily neglect the effect of θ_{34} and δ_{34} in the analysis, if one does not consider matter effect and neutral current events.

The appearance channel probability $[\mathrm{P}(\nu_\mu \to \nu_e)]$ is an important channel to verify the active neutrino oscillations to sterile neutrino at the near detector. As our beam consists of muon type neutrinos, we do not expect any significant signal of electron type neutrinos above the known

[1]Note that throughout our text we have used the notation δ_{CP} for δ_{13}.

background as the neutrinos at the near detector will be unoscillated due to insufficient distance for oscillation to occur. If significant excess of electron type neutrinos are detected at the near detector, it may indicate the presence of sterile neutrino, that oscillates to active electron type neutrinos. The appearance channel probability of neutrinos in effective two flavor approximation with an extra light sterile neutrino at the near detector can be found in Refs. [31,37–39]:

$$P_{\mu e}^{\mathrm{ND}} = \sin^2 2\theta_{14} \sin^2 \theta_{24} \sin^2\left(\frac{\Delta m_{41}^2 L}{4E_\nu}\right), \tag{3}$$

where θ_{14} and θ_{24} are sterile mixing angles, Δm_{41}^2 is the sterile mass squared difference, E_ν is neutrino energy and L is the baseline length. As we can see the probability term is dependent on the sterile oscillation parameters only, hence the near detector facilitates the best platform to study the sterile neutrinos.

The approximate appearance channel probability at the far detector which was calculated for the first time in Ref. [38], is given by

$$\begin{aligned} P_{\mu e}^{\mathrm{FD}} &= 4 s_{13}^2 s_{23}^2 \sin^2 \Delta_{31} \\ &\quad + 8 s_{12} c_{12} s_{13} s_{23} c_{23} \sin \Delta_{21} \sin \Delta_{31} \cos(\Delta_{31} + \delta_{CP}) \\ &\quad + 4 s_{13} s_{14} s_{24} s_{23} \sin \Delta_{31} \sin(\Delta_{31} + \delta_{CP} + \delta_{24}), \end{aligned} \tag{4}$$

where $\Delta_{ij} = \frac{\Delta m_{ij}^2 L}{4E}$. To arrive at this expression one needs to use the long baseline approximations ($\Delta_{21} \to 0$ and $\Delta_{41} \to \infty$). It should be noted that the probability expression in Eq. (4) does not depend on Δm_{41}^2. The reason being, for the L/E values relevant for far detectors, the oscillations are averaged out for any particular value of Δm_{41}^2. Therefore, this probability expression is independent of Δm_{41}^2. Again this expression is independent of θ_{34} and δ_{34}. But this will not be the case when we consider the interaction with matter as both θ_{34} and δ_{34} will be modified due to matter effect, affecting the oscillation probability. However, the parameters, θ_{34} and δ_{34} become more effective if the neutral current events are considered. This behavior has been first pointed out in the analytical treatment presented in Ref. [38] and successively verified in the numerical simulations performed in Ref. [40].

III. EXPERIMENTAL SETUP AND SIMULATION DETAILS

We have used GLoBES [41,42] software package to simulate DUNE and three configurations at KM3NeT. We have further used additional plugins of GLoBES to implement the sterile neutrino in our study [43].

For simulating the long-baseline experiments at KM3NeT, we have taken the three configurations from Refs. [15,44]. The Protvino accelerator contains a 1.5 km circumference U-70 synchrotron which produces 90 KW beam corresponding to 0.8×10^{20} protons on target (POT) per year for P2O and 450 KW beam corresponding to 4×10^{20} POT per year for upgraded P2O and P2SO configurations. For P2O and upgraded P2O experiments, the neutrinos will be detected at ORCA (Oscillation Research with Cosmics in the Abyss) far detector (FD) located in the Mediterranean Sea about 40 km off the coast of Toulon, France. It is located at a depth between 2450 m (the seabed depth) and 2250 m. The ORCA detector will contain 8 Mt sea water in total out of which 4 Mt would be its fiducial volume. This detector will be about 2595 km away from the neutrino source. We used the fluxes as given in Ref. [15] and shown in Fig. 1. In this figure, we have shown the components of $\nu_\mu/\bar{\nu}_\mu$, $\nu_e/\bar{\nu}_e$ fluxes in both positive and negative polarities. From these panels, we understand that the flux corresponding to signal (i.e., ν_μ in the positive polarity and $\bar{\nu}_\mu$ in the negative polarity) is higher as compared to flux corresponding to background. However, in Ref. [45], we showed that for P2O, the major background for the ν_e signal events arise from ν_μ misidentified as ν_e, neutral current (NC) events identified as ν_e

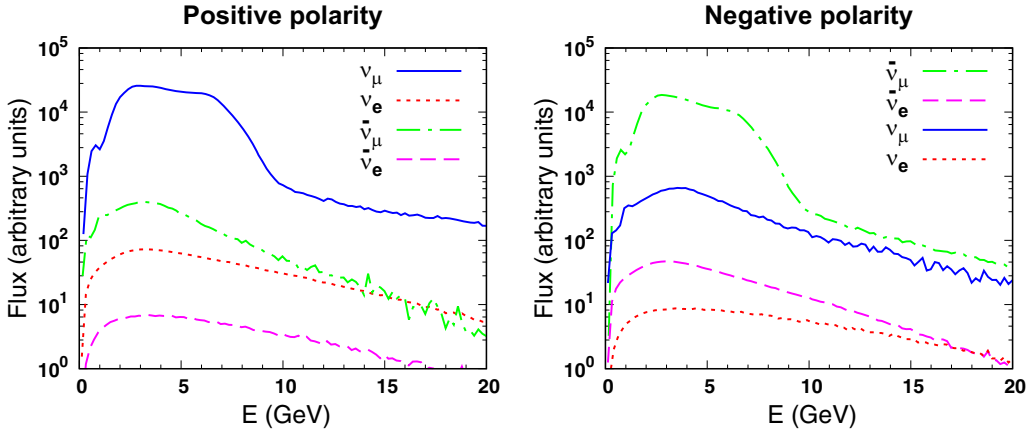

FIG. 1. Fluxes (in arbitrary units) as a function of neutrino energy for the P2O experiment.

and ν_τ identified as ν_e. This is because, the ORCA detector is mainly designed to detect atmospheric neutrinos and ultra high energy neutrinos from the extra-galactic sources. The electron events in the ORCA detector produce a shower. At 5 GeV, the efficiency of ν_e events classified as shower is 90%. But there are also 78% of the ν_τ events, 85% of the NC events and 50% of the ν_μ events classified as shower which act as a background for the ν_e selection [14]. We have included these backgrounds in our analysis. We employed presmearing energy dependant efficiencies to match the energy spectrum shown in Fig. 7 of Ref. [15]. These efficiencies account for the energy-dependent effective mass of the ORCA detector, as shown in Fig. 90 of Ref. [14]. The energy resolution and particle identification factor were obtained from Figs. 68 and 99 of Ref. [14]. We have checked that our physics sensitivity matches with Figs. 8 and 10 of Ref. [15] corresponding to P2O and upgraded P2O, respectively.

The Super-ORCA detector for the P2SO experiment will be 10 times denser than the ORCA detector. In comparison to ORCA, the Super-ORCA detector would have a lower energy threshold for neutrino detection, improved neutrino flavor identification capacity, and higher energy resolution. Using presmearing energy dependant efficiencies, we matched the energy spectrum of P2SO as shown in Fig. 5 of Ref. [44] and the particle identification factor was taken from Fig. 1. Our results reproduce the physics sensitivity of P2SO as given in Figs. 13–15 of Ref. [15]. We have considered a total run-time of six years, divided into three years in neutrino mode and three years in antineutrino mode for all three configurations of the long-baseline options at KM3NeT. The energy window for calculation of events is 2 GeV to 12 GeV for P2O/upgraded P2O and 0.2 GeV to 10 GeV in P2SO.

We utilized the official GLoBES files corresponding the technical design report [46] for DUNE. A 40 kt liquid argon time-projection chamber detector with a beam power of 1.2 MW and a running time of 7 years is positioned 1300 km away from the source, producing 1.1×10^{21} POT per year. The run-time has been divided into 3.5 years in neutrino mode and 3.5 years in antineutrino mode. The neutrino source will be located in Fermilab in the United States, and the detector will be located in South Dakota.

Now let us discuss about the configuration of the near detectors (ND). For DUNE, we have considered an identical detector as that of far detector having volume of 0.147 kt at a distance of 574 m from the source. For KM3NeT, we have used a DUNE like near detector placed at a distance of 320 m from the source. Here we have taken the detector volume in such a way that the number of signal events at the near detector for DUNE and the number of signal events at the near detector for P2O match with each other for $\Delta m^2_{41} = 1$ eV^2. This way we ensure that the sensitivities coming from the near detector of DUNE and near detector of P2O are comparable.

TABLE I. The values of oscillation parameters that we considered in our analysis. Standard oscillation parameters are taken from [1] with their corresponding 1σ errors.

Parameters	True values $\pm 1\sigma$
$\sin^2\theta_{12}$	$0.304^{+0.013}_{-0.012}$
$\sin^2\theta_{13}$	$0.0222^{+0.00068}_{-0.00062}$
$\sin^2\theta_{23}$	$0.573^{+0.018}_{-0.023}$
$\delta_{\mathrm{CP}}[^\circ]$	194^{+52}_{-25}
Δm^2_{21} [10^{-5} eV^2]	$7.42^{+0.21}_{-0.20}$
Δm^2_{31} [10^{-3} eV^2]	$2.515^{+0.028}_{-0.028}$
$\sin^2\theta_{14}$	0.0076
$\sin^2\theta_{24}$	0.0076
$\sin^2\theta_{34}$	0
$\delta_{24}[^\circ]$	0
$\delta_{34}[^\circ]$	0
Δm^2_{41} [eV^2]	0.1, 1, 10

For the estimation of the sensitivity, we use the Poisson log-likelihood and assume that it is χ^2-distributed:

$$\chi^2_{\mathrm{stat}} = 2\sum_{i=1}^{n}\left[N_i^{\mathrm{test}} - N_i^{\mathrm{true}} - N_i^{\mathrm{true}}\log\left(\frac{N_i^{\mathrm{test}}}{N_i^{\mathrm{true}}}\right)\right], \quad (5)$$

where N^{test} is the number of events in the test spectrum, N^{true} is the number of events in the true spectrum and i is the number of energy bins. The best-fit values of the oscillation parameters and their 1σ errors are taken from NuFIT [1] and are listed in Table I. In our analysis, we have marginalized over all the relevant parameters using the built-in minimizer in GLoBES taking a prior corresponding to their 1σ uncertainty. For δ_{CP} and the sterile oscillation parameters, we have not considered any priors and they are allowed to vary freely. The systematic is incorporated by the pull method [47,48]. For systematic errors, we have taken an overall normalization and shape errors corresponding to signal and background. We list the values of the systematic errors for KM3NeT and DUNE in Table II. It should be noted that the DUNE GLoBES file contains no shape errors. We show all our results for the normal hierarchy of the neutrino masses.

IV. DISCUSSION AT THE PROBABILITY LEVEL

In Fig. 2, we have shown the appearance channel probability as a function of neutrino energy for different values of Δm^2_{41}. The left plot is for DUNE near detector which is placed at 574 meters from the neutrino beam source and the right plot is for P2O near detector which is placed at 320 meters from the source. The red and blue curves correspond to $\Delta m^2_{41} = 1$ eV^2 and 10 eV^2, respectively. The black curves correspond to the neutrino fluxes in arbitrary units. Both the experiments are insensitive to

TABLE II. The values of systematic errors that we considered in our analysis. "norm" stands for normalization error, "Sg" stands for signal and "Bg" stands for background.

Systematics	P2O	Up P2O	P2SO	DUNE
Sg-norm ν_e	7%	7%	5%	2%
Sg-norm ν_μ	5%	5%	5%	5%
Bg-norm	12%	12%	12%	5% to 20%
Sg-shape	11%	11%	11%	NA
Bg-shape	4% to 11%	4% to 11%	4% to 11%	NA

sterile neutrino mass squared difference of $\Delta m^2_{41} = 0.1\ \mathrm{eV}^2$, which we have not shown here. Next we see that most part of the red curve lies inside the flux envelop for DUNE near detector but this is not the case for the P2O near detector. From this we can draw an important conclusion that the DUNE experiment will be more sensitive to $\Delta m^2_{41} = 1\ \mathrm{eV}^2$ sterile neutrinos. The first maxima for $\Delta m^2_{41} = 10\ \mathrm{eV}^2$ coincides with the flux maxima of P2O experiment whereas second maxima and some part of first maxima lies inside the flux envelop of DUNE experiment. Therefore, we can expect that P2O experiment will provide best sensitivity to $\Delta m^2_{41} = 10\ \mathrm{eV}^2$ sterile neutrinos.

V. CONSTRAINING STERILE OSCILLATION PARAMETERS

In this section, we will estimate the bound on the different sterile mixing parameters assuming there are no light sterile neutrinos in nature.

In Fig. 3, we have shown the allowed region for the sterile oscillation parameters $\sin^2\theta_{14}$ and $\sin^2\theta_{24}$ at 95% confidence level. The upper (lower) panel corresponds to the case where ND + FD (FD) configuration was considered for constraining these parameters. The different colors correspond to various experiments. The blue curve represents the allowed region for DUNE experiment, while green, red, and yellow bands represent the regions for P2O, upgraded P2O, and P2SO experiments, respectively. Left, middle, and right columns in the figure represent three different values of the sterile mass squared differences $\Delta m^2_{41} = 0.1\ \mathrm{eV}^2$, $1\ \mathrm{eV}^2$, and $10\ \mathrm{eV}^2$, respectively. If we compare the lower panel with the upper panel, we can identify that the FD + ND configurations are giving more stringent bounds on the sterile mixing angles compared to the case where only FD is considered except the case for $\Delta m^2_{41} = 0.1\ \mathrm{eV}^2$. The reason for the enhancement in the ND + FD scenario is because of the fact that ND exhibit higher sensitivity to oscillations caused by sterile neutrinos ($\Delta m^2_{41} = 1\ \mathrm{eV}^2$ and $10\ \mathrm{eV}^2$) compared to FD cases alone, as the latter experience frequency averaging due to rapid oscillations. As discussed earlier, for $\Delta m^2_{41} = 0.1\ \mathrm{eV}^2$ NDs of P2O and DUNE experiments are insensitive to sterile neutrinos and for this reason, adding a ND does not help in the improvement in the sensitivity. If we focus on the case for $\Delta m^2_{41} = 1\ \mathrm{eV}^2$, we can clearly see that DUNE experiment gives the best bound for the ND + FD configuration and if we shift our focus to the case for $\Delta m^2_{41} = 10\ \mathrm{eV}^2$, we can see that P2SO and upgraded P2O configurations are giving best bound on the sterile parameters. This observation can be well understood from Fig. 2. We can see one more interesting feature in these two plots that the P2SO and upgraded P2O bands are overlapping for the ND + FD case. This is due to the fact that the NDs for both P2SO and upgraded P2O are the same in terms of both beam exposure and running period. The sensitivity of P2O is inferior than upgraded P2O and P2SO but better than DUNE for $\Delta m^2_{41} = 10\ \mathrm{eV}^2$ and FD + ND. In the case of FD only, as we change the value of Δm^2_{41} we do not see any significant change in the bounds for all the experiments. This is due to the fact that the appearance channel probability, Eq. (3) does not depend on Δm^2_{41} when we consider FD only. Note that the current bounds on the sterile mixing angles are available from the ongoing

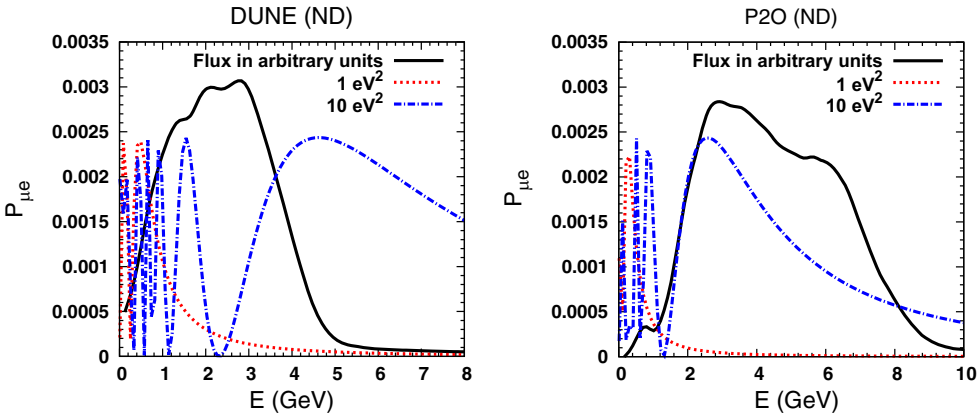

FIG. 2. Electron neutrino appearance probability as a function of energy for DUNE and P2O near detectors for Δm^2_{41} as $1\ \mathrm{eV}^2$ and $10\ \mathrm{eV}^2$. Also we have shown the corresponding fluxes of the experiments in probability plot.

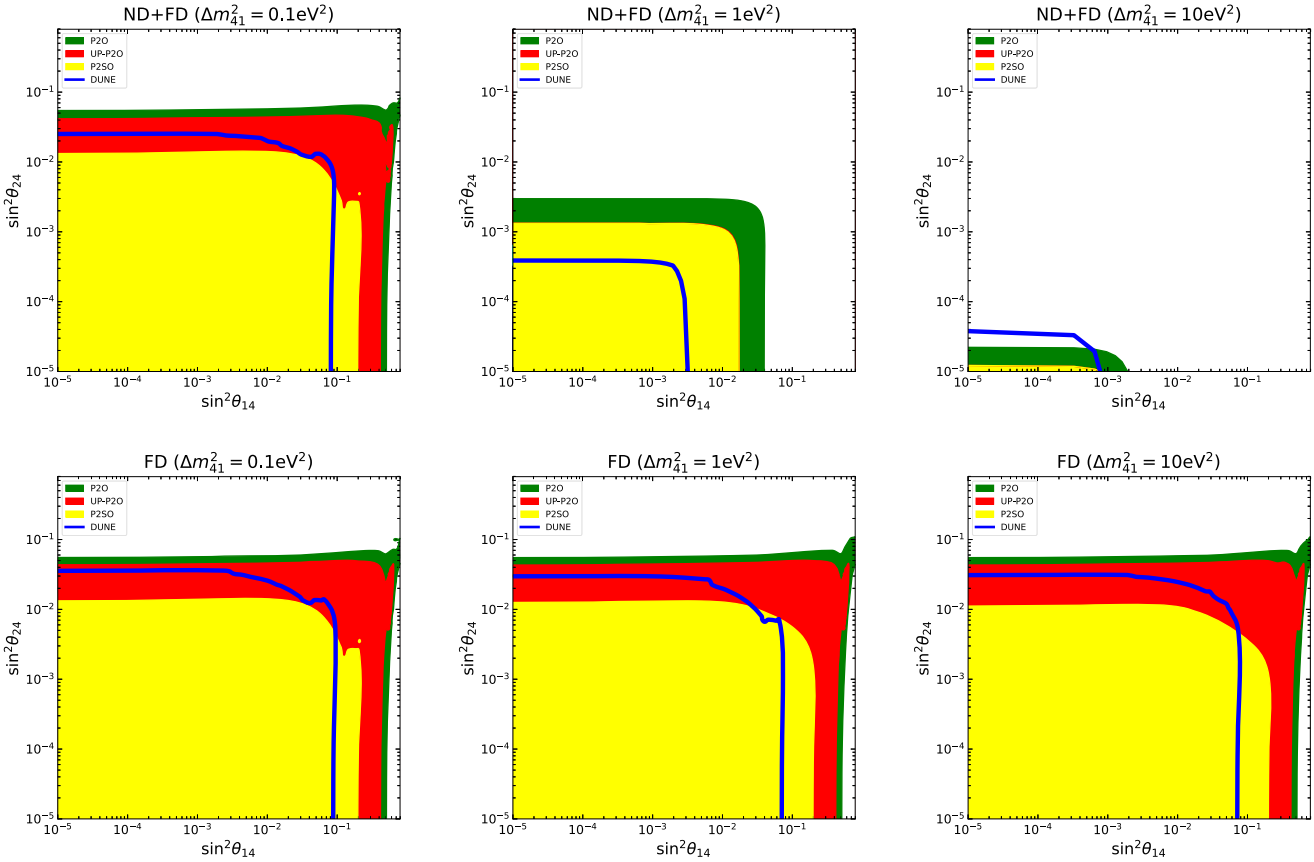

FIG. 3. Capability of DUNE, P2O, upgraded P2O, and P2SO to constrain the sterile neutrino parameters θ_{14} and θ_{24}. In the upper (lower) panel we present the two-dimensional sensitivity curves in $\sin^2\theta_{14}$–$\sin^2\theta_{24}$ plane for ND + FD (FD) at 95% C.L.

experiments [49]. But our results cannot be compared with theirs as they are obtained using a different parametrization of the PMNS matrix.

VI. HIERARCHY SENSITIVITY

The sensitivities to neutrino mass hierarchy for different long-baseline experiments in standard three flavor and in the presence of sterile neutrino have been shown in Fig. 4. Each column represents the sensitivity from χ^2_{min} to χ^2_{max} arising due to the different values of true δ_{CP}. Hierarchy sensitivity is the capability of the experiment to exclude the wrong hierarchy. In order to calculate hierarchy sensitivity, we obtain χ^2 assuming true hierarchy as NH and test hierarchy as IH. The upper panel represents the situation where both ND and FD were included for the study, whereas the lower panel corresponds to the FD case only. The red bars represent the hierarchy sensitivity in standard three flavor scenario and the blue bars represent the case with one extra sterile neutrino. In each row, the left panel corresponds to $\Delta m^2_{41} = 1$ eV^2 and the right panel corresponds to $\Delta m^2_{41} = 10$ eV^2.

As we know the hierarchy sensitivity is directly proportional to the matter effect, i.e., higher the baseline, higher the hierarchy sensitivity. Holding on to that logic, we would expect that P2O experiment (all three configurations) should provide more sensitivity to hierarchy. As we can see from the figure that in standard interaction case P2SO gives the best sensitivity to mass hierarchy, whereas DUNE and upgraded P2O give the next best sensitivity. P2O is least sensitive to hierarchy due to its low background rejection capability and 5 time less beam power compared to upgraded P2O and P2SO. We have shown this fact in our previous work [45]. We can notice that the upgraded P2O sensitivity to mass hierarchy is less than the P2SO sensitivity although their baseline and beam power are same. This is due to the fact that upgraded P2O uses ORCA detector with limited background rejection capability compared to the improved Super-ORCA detector used by P2SO.

In the presence of a sterile neutrino, the hierarchy sensitivities of all the experiments decrease due to the degeneracies arising between standard oscillation parameters with the sterile mixing angles and sterile phases. As the FDs are not sensitive to the sterile neutrinos, the hierarchy sensitivities of all the experiments are low. There is no significant difference when we change the sterile mass squared difference Δm^2_{41} from 1 eV^2 to 10 eV^2. Once we introduce the NDs, we find an improvement in their

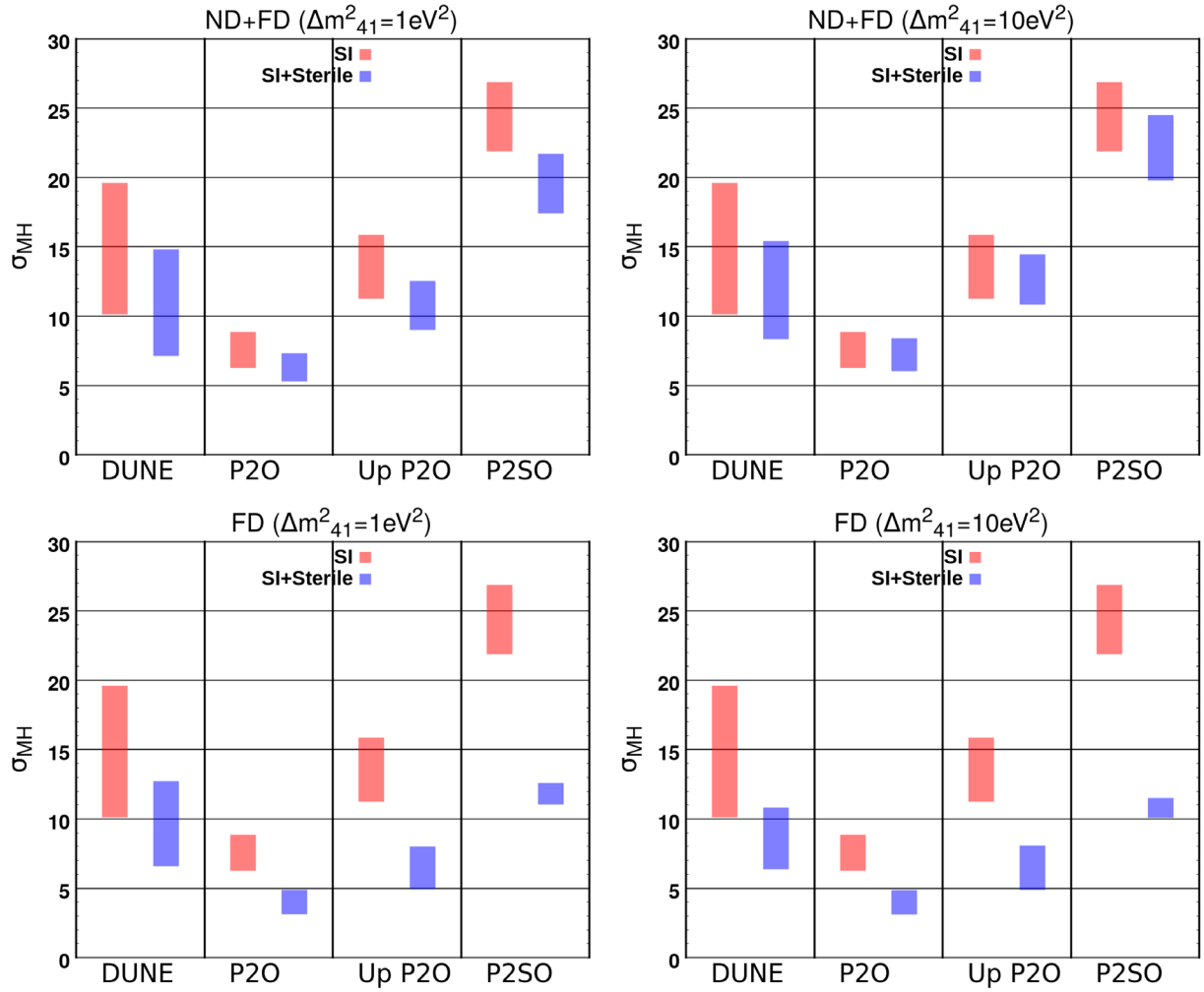

FIG. 4. Range of MH sensitivities of DUNE, P2O, upgraded P2O (Up P2O) and P2SO for the standard interaction (SI) case as well as SI + sterile case for $\Delta m^2_{41} = 1$ eV^2 and 10 eV^2.

sensitivities. This is because, inclusion of ND provides a constraint on the sterile mixing parameters which are free in case of only FD. For P2O, upgraded P2O, and P2SO, the improvement in the sensitivity is more in the case of $\Delta m^2_{41} = 10$ eV^2 as compared to $\Delta m^2_{41} = 1$ eV^2. For DUNE, the improvement is same for both $\Delta m^2_{41} = 10$ eV^2 and 1 eV^2. The hierarchy sensitivity of upgraded P2O in the presence of sterile neutrino is comparable to DUNE both for $\Delta m^2_{41} = 1$ eV^2 and $\Delta m^2_{41} = 10$ eV^2. Similar to the standard interaction case P2O gives the least sensitivity to hierarchy in the presence of sterile neutrino.

VII. OCTANT SENSITIVITY

In Fig. 5, we have shown the region of $\sin^2\theta_{23}$ in the range [0.4:0.62], where the true octant can be determined above 3σ C.L. for DUNE, upgraded P2O and P2SO experiments in the standard three flavor scenario and in presence of sterile neutrino. Octant sensitivity represents the capability of the experiment to exclude the degenerate solutions for θ_{23} if any exists. In order to calculate octant sensitivity, we obtain χ^2 assuming the true θ_{23} in LO and varying the test θ_{23} in HO and vice versa. In each panel, red (blue) band represents the range of $\sin^2\theta_{23}$ in LO having octant sensitivity greater than 3σ in the standard (SI + sterile) scenario. Similarly green (cyan) band represents the range of $\sin^2\theta_{23}$ for HO in the standard (presence of sterile) neutrino scenario. Upper panel of the figure represents the sensitivities considering the combination of ND and FD for each long baseline experiment, while plots in lower panel show the octant sensitivities with only FD. Each plot on the left panel displays octant sensitivities assuming the new mass squared difference Δm^2_{41} as 1 eV^2, while the right panel plots are obtained for Δm^2_{41} as 10 eV^2.

The sensitivities to octant degeneracy are relatively weak and below 3σ for almost whole range of θ_{23} for P2O experiment, hence not shown in the figure. The upgraded P2O experiment has some octant sensitivity above 3σ only in standard interaction case, while no such sensitivity is obtained for sterile neutrino. DUNE and P2SO experiments

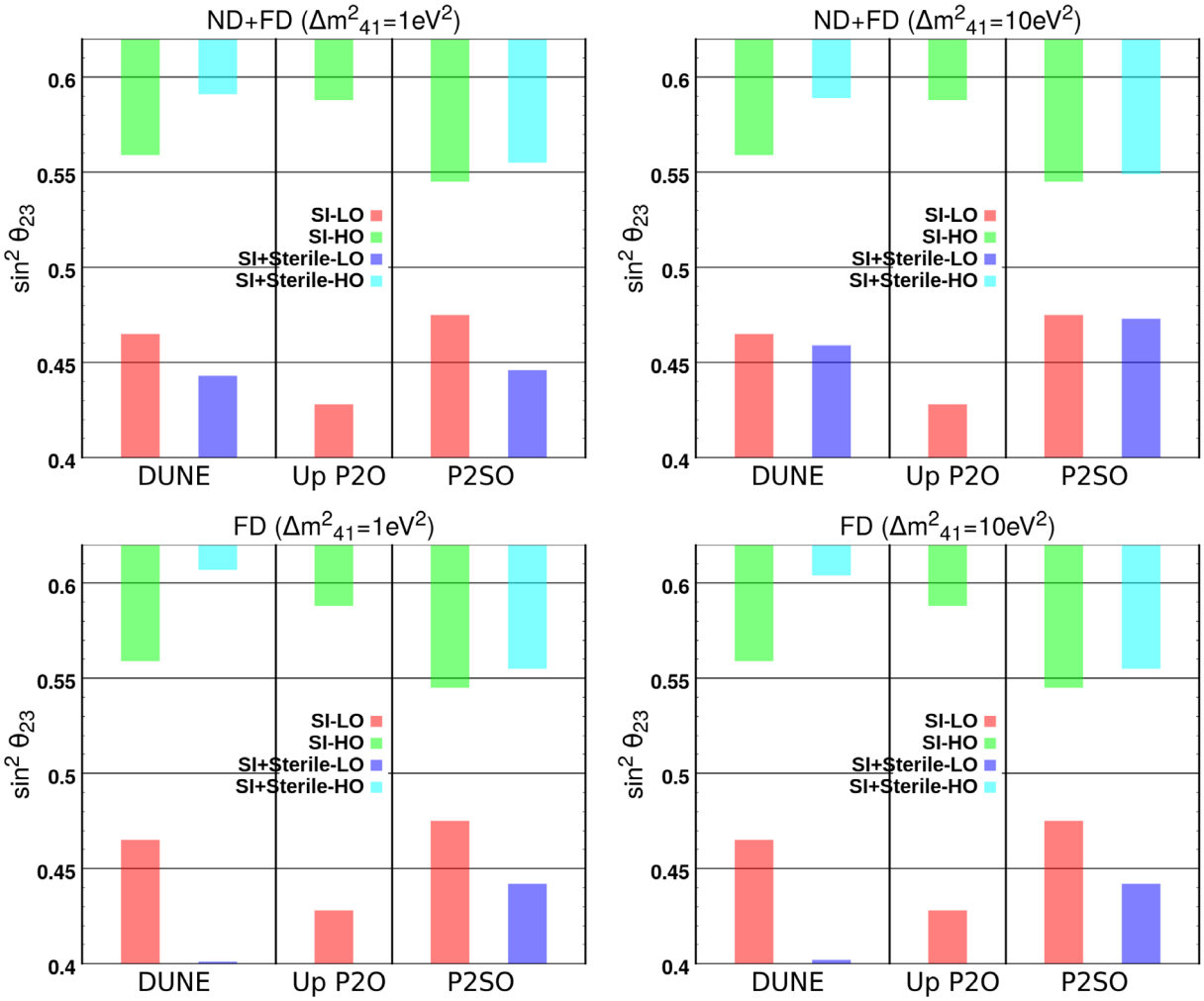

FIG. 5. Region of $\sin^2\theta_{23}$ for which octant can be determined above 3σ C.L. for DUNE, upgraded P2O (Up P2O), and P2SO experiments in standard interaction (SI) case and SI + sterile case for sterile neutrinos of masses $\Delta m^2_{41} = 1$ eV^2 and 10 eV^2.

are more sensitive to octant of θ_{23}. One can easily observe deterioration in octant sensitivity with only FD for all the experiments after including the sterile neutrino to the standard three flavor scenario. Another crucial observation is related to the contribution of ND in each experiment. As discussed earlier, ND is more important for analysis of sterile neutrino. Hence, inclusion of ND to FD in each experiment enhances the sensitivity significantly. But for P2SO experiment (blue band) there is notable increment in region for LO, while for HO region no such change in sensitivity is observed after including ND to FD as compared to only FD. In order to understand this anomalous result from P2SO, we have calculated the values of different oscillation parameters at the minimum χ^2_{min} values corresponding to θ_{23} in LO and HO regions. Interestingly for θ_{23} in LO, we observed that the parameters θ_{34} and δ_{34} are more constrained in FD + ND compared to only FD. No such observations are found for HO. For further clarification we have removed the dependency on θ_{34} and δ_{34} by assuming their values to be zero and obtained no such anomalous octant sensitivities. This implies the fact that there exists some degeneracies involving the sterile parameters θ_{34} and δ_{34}. As a result for LO, both θ_{34} and δ_{34} are unconstrained with only FD. ND helps to tightly constrain these parameters in LO regions. FD is quite effective to constrain θ_{34} and δ_{34} in HO region and hence we observed no such effect for ND in HO region.

VIII. *CP* VIOLATION SENSITIVITY

The oscillation parameter δ_{CP} is bit slow as compared to other oscillation parameters in the race of precise measurement of them. The parameter δ_{CP} has great importance to explain the *CP* violation in neutrino sector and also can explain the matter and antimatter asymmetry of the universe. In order to show the potential to find *CP* violation in nature, we have calculated *CP* violation (CPV) sensitivities for different long-baseline experiments. CPV sensitivity shows the ability of the experiment to exclude the *CP* conserving values of δ_{CP}, if *CP* violation exists. In order to

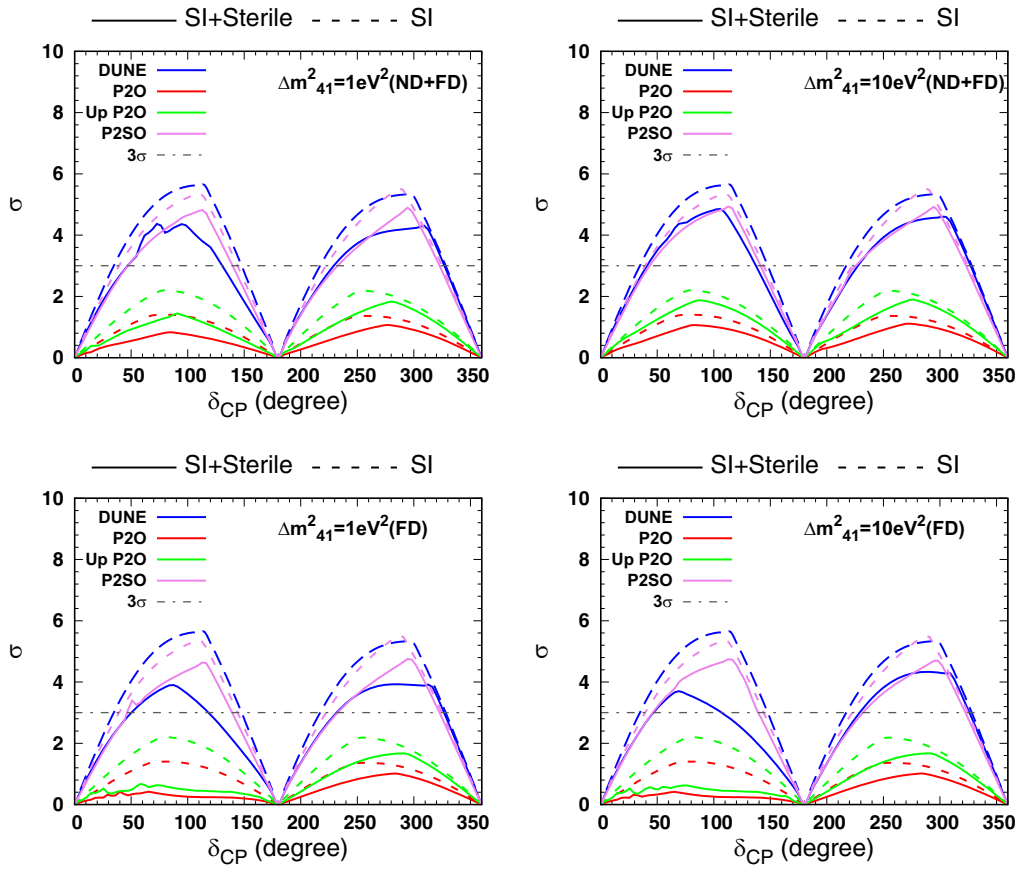

FIG. 6. CPV sensitivities as a function of true δ_{CP} for DUNE, P2O, upgraded P2O (Up P2O), and P2SO experiments in Standard Interaction (SI) case and SI + Sterile case for sterile neutrinos of masses $\Delta m^2_{41} = 1$ eV^2 and 10 eV^2.

calculate CP violation sensitivity, we obtain χ^2 assuming the CP conserving values in test and minimizing over them. Figure 6 displays the CPV sensitivities as a function of true δ_{CP} for standard and in presence of sterile neutrino in dashed and solid curves, respectively. Plots on the left panel of the figure show the sensitivities with sterile neutrino of $\Delta m^2_{41} = 1$ eV^2 while the right panel is for sterile neutrino of $\Delta m^2_{41} = 10$ eV^2. Upper panel (lower panel) represents the CPV sensitivities with ND + FD (FD). In each plot the different colored curves, i.e., blue, red, green and magenta represent the CPV sensitivities for DUNE, P2O, upgraded P2O, and P2SO experiments, respectively.

As expected, in SI scenario (dashed curve) higher CPV sensitivity values are obtained around the maximum CP violating values (90° and 270°) of δ_{CP} and lowest sensitivities are at CP conserving values. The long-baseline experiments P2O and upgraded P2O are less significant toward CP violation as the sensitivities are below 3σ for the whole region of δ_{CP}. The reason for lower CPV sensitivities is the low background rejection capability of both the experiments. DUNE and P2SO experiments are more sensitive toward CP violation and can able to establish CP violation at 3σ C.L., if it exists in nature. Addition of sterile neutrino to three neutrino scenario results to decrease in minimum CPV sensitivities (solid curves) for all the experiments. Also, effect of ND in each experiment is clearly visible. After including ND to FD, significant increase in sensitivities is observed, compared to only FD in each experiment in 3 + 1 scenario for δ_{CP} in the region 0° to 180°. We can see that, in presence of sterile neutrino there is no significant improvement of CPV sensitivity in the region 180° to 360° of δ_{CP} after adding ND to the FD. This feature can be explained in a similar fashion as the octant case. Note that the CP violation in presence of sterile neutrino is not only due to the standard CP phase, but can also be due to the sterile phases. By varying the δ_{24} and δ_{34} in their allowed ranges, one can get bands instead of a single curve, by calculating maximum and minimum values of $\Delta\chi^2_{\text{min}}$ as shown in Ref [33]. Sterile phases can enhance or deteriorate CPV sensitivity depending upon their values. In the next section, we have shown the effects of δ_{24} on the measurement of δ_{CP}.

IX. CONSTRAINING CP PHASES

As discussed in the previous section, additional CP phases can be the reason for CP violation. In this section, we have shown CP precision sensitivities for long baseline experiments DUNE and P2SO as shown in Fig. 7. In our

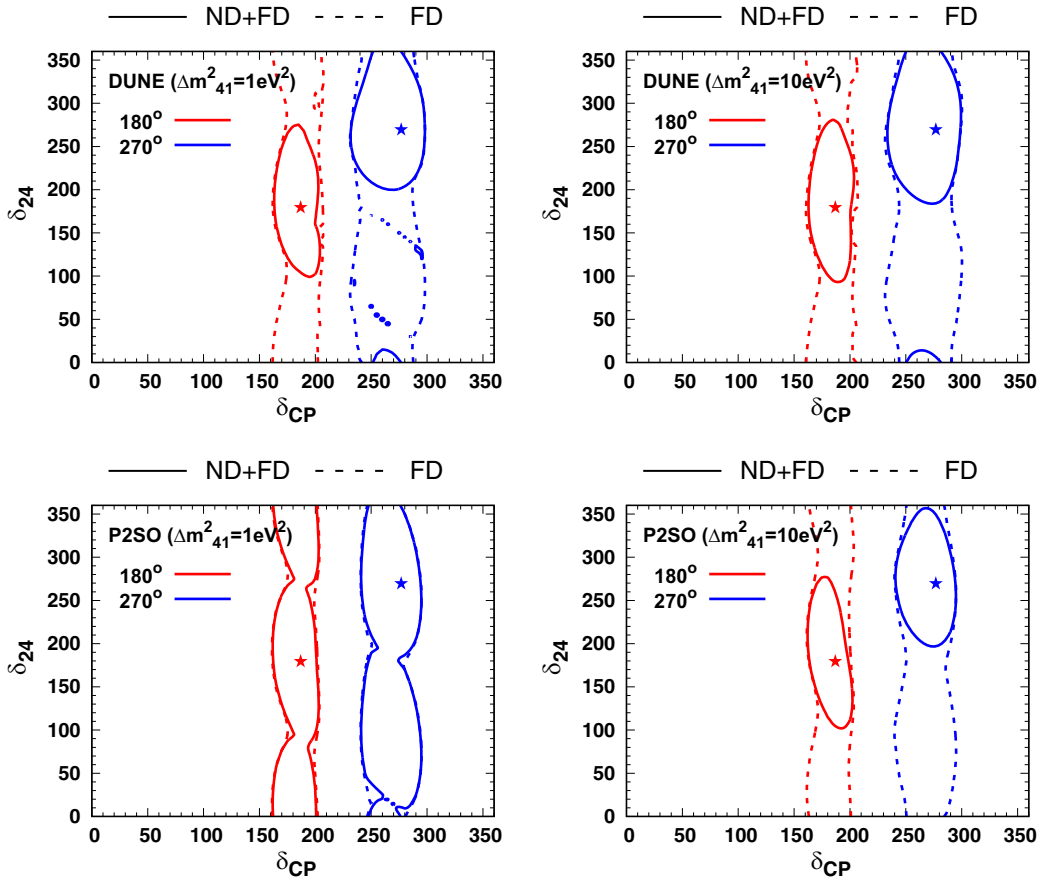

FIG. 7. *CP* precision sensitivity in δ_{CP} and δ_{24} plane for DUNE and P2SO experiments. We have shown the sensitivity at 1σ C.L. in presence of a light sterile neutrino of masses $\Delta m^2_{41} = 1$ eV^2 and 10 eV^2.

study, we have not considered P2O and upgraded P2O because they have limited sensitivity to δ_{CP}. *CP* precision sensitivity says how precisely one can measure a particular value of *CP* phase. In our analysis, we have estimated the *CP* precision sensitivity, considering *CP* conserving or maximal *CP* violating values for the *CP* phases δ_{CP} and δ_{24}, i.e., for the true combination of (δ_{CP}, δ_{24}) of (180°, 180°) and (270°, 270°). Note that *CP* precision in $3+1$ scenario can be studied for many combinations of (δ_{CP}, δ_{24}). Our choice for the values of *CP* phases is motivated by the recent measurement of δ_{CP} by T2K [50] and NOνA [51]. The measurement of T2K gives a best-fit value of δ_{CP} around the maximal *CP* violating value of 270° whereas the current best-fit value of this parameter by NOνA is around the *CP* conserving value of 180°. Marginalization has been done over all standard and sterile oscillation parameters except the mass squared difference Δm^2_{41}. Left (right) panel of the figure shows the sensitivity with sterile neutrino mass order of 1 eV^2 (10 eV^2). Upper panel is for DUNE experiment while lower panel is for P2SO experiment. In each plot, the dashed (solid) curve represents the allowed region between δ_{CP} and δ_{24} at 1σ C.L. considering FD (ND + FD). Red and blue color of the curves represent the true value of *CP* phases δ_{CP} and δ_{24} as 180° and 270°, respectively. Star marks in each plot show the true point considered for analysis.

As expected the inclusion of ND to FD increases the sensitivities of the experiments as compared to only FD except for the case of P2SO and $\Delta m^2_{41} = 1$ eV^2. Due to the effect of ND, parameter spaces (specially the sterile angles) are more constrained and experiments can measure the *CP* conserving and *CP* violating values of the *CP* phases with great accuracy. For P2SO and $\Delta m^2_{41} = 1$ eV^2, addition of ND does not improve the sensitivity. This is because, in this case, the flux is optimal for $\Delta m^2_{41} = 10$ eV^2 at the ND. For $\Delta m^2_{41} = 10$ eV^2, both the experiments can equally measure the *CP* violating and *CP* conserving values of the phases. Note that for the measurement of phases in $3+1$ scenario, it would be ideal to have a ND capable of detecting ν_τ via $\nu_\mu \to \nu_\tau$ [52]. However, even without the capability of τ neutrino detection, having a replica of the far detector at a short distance, one can keep the systematics under control and measure the phases at a good precision.

X. SUMMARY AND CONCLUSIONS

In this paper we have studied the capability of the long-baseline experiment options at the KM3NeT facility to

probe the light sterile neutrino. In our study, we have considered the options P2O, which will have neutrinos from a 90 KW beam to be detected at the ORCA detector, the upgraded P2O, which will have neutrinos from the upgraded 450 KW beam to be detected at the ORCA detector and the option of P2SO, which will have neutrinos from a 450 KW beam to be detected at the upgraded Super-ORCA detector. All these options will have a baseline around 2595 km. We have also compared the results of these three options with DUNE.

In our study, we showed that the options at the KM3NeT is more sensitive if the value of Δm^2_{41} is around 10 eV^2 whereas the DUNE is more sensitive if the value of Δm^2_{41} is around 1 eV^2. Our results also show that near detector is very important for the study of sterile neutrinos and addition of near detector improves the sensitivity as compared to only far detector for $3+1$ scenario. Among the three options at KM3NeT, the sensitivities of P2O and upgraded P2O are limited because of their poor background rejection capabilities. Regarding the capability of constraining the sterile mixing parameters, we find that both P2SO and DUNE have good efficiency to constrain the mixing angles θ_{14} and θ_{24}. DUNE is better for $\Delta m^2_{41} = 1$ eV^2 while P2SO is better for $\Delta m^2_{41} = 10$ eV^2. The sensitivities of P2SO and upgraded P2O are exactly same for ND + FD configuration. Regarding determination of the unknowns in $3+1$ scenario, we find that the sensitivities in presence of sterile neutrino is lower as compared to standard three flavor case. Addition of ND improves the sensitivities but still they are less than the standard three flavor case. In general, we have observed that, for $\Delta m^2_{41} = 10$ eV^2, improvement in the sensitivity due to the addition of ND is more for the long-baseline experiment options at KM3NeT as compared to $\Delta m^2_{41} = 1$ eV^2. Regarding hierarchy sensitivity in presence of sterile neutrinos, sensitivity of upgraded P2O is similar to DUNE whereas P2SO gives the best sensitivity for ND + FD. Regarding octant and CP sensitivities, we find that the sensitivities of P2O and upgraded P2O are poor compared to DUNE and P2SO in the $3+1$ scenario and for ND + FD. For octant, the best sensitivity comes from P2SO and for δ_{CP}, DUNE provides slightly better sensitivity than P2SO regarding both CP violation and CP precision. We find that addition of ND does not play any role in the case of (i) octant sensitivity in the higher octant for P2SO, (ii) CPV sensitivity in the 180° to 360° region of δ_{CP} for all the experimental setups, and (iii) CP precision sensitivity for $\Delta m^2_{41} = 1$ eV^2 for P2SO.

In summary, our results show that the sensitivity of P2SO, i.e., the long-baseline option of KM3NeT where neutrinos from a 450 KW beam at Protvino will be detected at the Super-ORCA detector, is either comparable or better than DUNE in both standard and $3+1$ scenario. Our results will help in the design of the long-baseline experiments at KM3NeT facility.

ACKNOWLEDGMENTS

D. K. S. acknowledges Prime Minister's Research Fellowship, Government of India. M. G. acknowledges Ramanujan Fellowship of SERB, Government of India, through Grant No. RJF/2020/000082. R. M. acknowledges the support from University of Hyderabad through the IoE Project Grant No. IoE/RC1/RC1-20-012. We acknowledge the use of CMSD HPC facility of University of Hyderabad to carry out computations in this work. This work has been in part funded by Ministry of Science and Education of Republic of Croatia Grant No. KK.01.1.1.01.0001.

[1] I. Esteban, M. C. Gonzalez-Garcia, M. Maltoni, T. Schwetz, and A. Zhou, The fate of hints: Updated global analysis of three-flavor neutrino oscillations, J. High Energy Phys. 09 (2020) 178.

[2] M. A. Acero *et al.*, White paper on light sterile neutrino searches and related phenomenology, arXiv:2203.07323.

[3] A. Aguilar-Arevalo *et al.* (LSND Collaboration), Evidence for neutrino oscillations from the observation of $\bar{\nu}_e$ appearance in a $\bar{\nu}_\mu$ beam, Phys. Rev. D **64**, 112007 (2001).

[4] A. A. Aguilar-Arevalo *et al.* (MiniBooNE Collaboration), Updated MiniBooNE neutrino oscillation results with increased data and new background studies, Phys. Rev. D **103**, 052002 (2021).

[5] C. Giunti, Y. F. Li, C. A. Ternes, and Z. Xin, Reactor antineutrino anomaly in light of recent flux model refinements, Phys. Lett. B **829**, 137054 (2022).

[6] M. A. Acero, C. Giunti, and M. Laveder, Limits on nu(e) and anti-nu(e) disappearance from Gallium and reactor experiments, Phys. Rev. D **78**, 073009 (2008).

[7] P. Abratenko *et al.* (MicroBooNE Collaboration), Search for an Excess of Electron Neutrino Interactions in MicroBooNE Using Multiple Final-State Topologies, Phys. Rev. Lett. **128**, 241801 (2022).

[8] P. B. Denton, Sterile Neutrino Search with MicroBooNE's Electron Neutrino Disappearance Data, Phys. Rev. Lett. **129**, 061801 (2022).

[9] P. Abratenko *et al.* (MicroBooNE Collaboration), First Constraints on Light Sterile Neutrino Oscillations from Combined Appearance and Disappearance Searches with the MicroBooNE Detector, Phys. Rev. Lett. **130**, 011801 (2023).

[10] A. A. Aguilar-Arevalo *et al.* (MiniBooNE Collaboration), MiniBooNE and MicroBooNE Combined Fit to a $3+1$

Sterile Neutrino Scenario, Phys. Rev. Lett. **129**, 201801 (2022).
[11] V. V. Barinov *et al.*, Results from the Baksan Experiment on Sterile Transitions (BEST), Phys. Rev. Lett. **128**, 232501 (2022).
[12] A. P. Serebrov *et al.*, Search for sterile neutrinos with the Neutrino-4 experiment and measurement results, Phys. Rev. D **104**, 032003 (2021).
[13] M. G. Aartsen *et al.* (IceCube Collaboration), eV-Scale Sterile Neutrino Search Using Eight Years of Atmospheric Muon Neutrino Data from the IceCube Neutrino Observatory, Phys. Rev. Lett. **125**, 141801 (2020).
[14] S. Adrian-Martinez *et al.* (KM3NeT Collaboration), Letter of intent for KM3NeT 2.0, J. Phys. G **43**, 084001 (2016).
[15] A. V. Akindinov *et al.*, Letter of interest for a neutrino beam from Protvino to KM3NeT/ORCA, Eur. Phys. J. C **79**, 758 (2019).
[16] B. Abi *et al.* (DUNE Collaboration), Deep underground neutrino experiment (DUNE), far detector technical design report, Volume II: DUNE Physics, arXiv:2002.03005.
[17] J. M. Berryman, A. de Gouvêa, K. J. Kelly, and A. Kobach, Sterile neutrino at the deep underground neutrino experiment, Phys. Rev. D **92**, 073012 (2015).
[18] R. Gandhi, B. Kayser, M. Masud, and S. Prakash, The impact of sterile neutrinos on *CP* measurements at long baselines, J. High Energy Phys. 11 (2015) 039.
[19] S. K. Agarwalla, S. S. Chatterjee, and A. Palazzo, Physics reach of DUNE with a light sterile neutrino, J. High Energy Phys. 09 (2016) 016.
[20] S. K. Agarwalla, S. S. Chatterjee, and A. Palazzo, Octant of θ_{23} in Danger with a Light Sterile Neutrino, Phys. Rev. Lett. **118**, 031804 (2017).
[21] J. T. Penedo and J. a. Pulido, Baseline and other effects for a sterile neutrino at DUNE, Phys. Rev. D **107**, 075026 (2023).
[22] P. Coloma, D. V. Forero, and S. J. Parke, DUNE sensitivities to the mixing between sterile and tau neutrinos, J. High Energy Phys. 07 (2018) 079.
[23] S. Choubey, D. Dutta, and D. Pramanik, Imprints of a light sterile neutrino at DUNE, T2HK and T2HKK, Phys. Rev. D **96**, 056026 (2017).
[24] S. Choubey, D. Dutta, and D. Pramanik, Measuring the sterile neutrino *CP* Phase at DUNE and T2HK, Eur. Phys. J. C **78**, 339 (2018).
[25] N. Haba, Y. Mimura, and T. Yamada, θ_{23} octant measurement in $3+1$ neutrino oscillations in T2HKK, Phys. Rev. D **101**, 075034 (2020).
[26] M. Ghosh, S. Gupta, Z. M. Matthews, P. Sharma, and A. G. Williams, Study of parameter degeneracy and hierarchy sensitivity of NOνA in presence of sterile neutrino, Phys. Rev. D **96**, 075018 (2017).
[27] S. Kumar Agarwalla, S. S. Chatterjee, and A. Palazzo, Physics potential of ESSνSB in the presence of a light sterile neutrino, J. High Energy Phys. 12 (2019) 174.
[28] R. Majhi, C. Soumya, and R. Mohanta, Light sterile neutrinos and their implications on currently running long-baseline and neutrinoless double beta decay experiments, J. Phys. G **47**, 095002 (2020).
[29] Y. Reyimuaji and C. Liu, Prospects of light sterile neutrino searches in long-baseline neutrino oscillations, J. High Energy Phys. 06 (2020) 094.
[30] M. Ghosh and R. Mohanta, Updated sensitivity of DUNE in $3+1$ scenario with far and near detectors, Eur. Phys. J. Special Topics **231**, 137 (2022).
[31] M. Ghosh, T. Ohlsson, and S. Rosauro-Alcaraz, Sensitivity to light sterile neutrinos at ESSnuSB, J. High Energy Phys. 03 (2020) 026.
[32] P. B. Denton, A. Giarnetti, and D. Meloni, How to identify different new neutrino oscillation physics scenarios at DUNE, J. High Energy Phys. 02 (2023) 210.
[33] D. Dutta, R. Gandhi, B. Kayser, M. Masud, and S. Prakash, Capabilities of long-baseline experiments in the presence of a sterile neutrino, J. High Energy Phys. 11 (2016) 122.
[34] S. Choubey, D. Dutta, and D. Pramanik, Exploring fake solutions in the sterile neutrino sector at long-baseline experiments, Eur. Phys. J. C **79**, 968 (2019).
[35] A. Donini, M. Maltoni, D. Meloni, P. Migliozzi, and F. Terranova, $3+1$ sterile neutrinos at the CNGS, J. High Energy Phys. 12 (2007) 013.
[36] F. Capozzi, C. Giunti, M. Laveder, and A. Palazzo, Joint short- and long-baseline constraints on light sterile neutrinos, Phys. Rev. D **95**, 033006 (2017).
[37] S. Böser, C. Buck, C. Giunti, J. Lesgourgues, L. Ludhova, S. Mertens, A. Schukraft, and M. Wurm, Status of light sterile neutrino searches, Prog. Part. Nucl. Phys. **111**, 103736 (2020).
[38] N. Klop and A. Palazzo, Imprints of *CP* violation induced by sterile neutrinos in T2K data, Phys. Rev. D **91**, 073017 (2015).
[39] J. Kopp, P. A. N. Machado, M. Maltoni, and T. Schwetz, Sterile neutrino oscillations: The global picture, J. High Energy Phys. 05 (2013) 050.
[40] R. Gandhi, B. Kayser, S. Prakash, and S. Roy, What measurements of neutrino neutral current events can reveal, J. High Energy Phys. 11 (2017) 202.
[41] P. Huber, M. Lindner, and W. Winter, Simulation of long-baseline neutrino oscillation experiments with GLoBES (General Long Baseline Experiment Simulator), Comput. Phys. Commun. **167**, 195 (2005).
[42] P. Huber, J. Kopp, M. Lindner, M. Rolinec, and W. Winter, New features in the simulation of neutrino oscillation experiments with GLoBES 3.0: General Long Baseline Experiment Simulator, Comput. Phys. Commun. **177**, 432 (2007).
[43] J. Kopp, Efficient numerical diagonalization of hermitian 3×3 matrices, Int. J. Mod. Phys. C **19**, 523 (2008).
[44] J. Hofestädt, M. Bruchner, and T. Eberl, Super-ORCA: Measuring the leptonic *CP*-phase with atmospheric neutrinos and beam neutrinos, *Proc. Sci.*, ICRC2019 (2020) 911 [arXiv:1907.12983].
[45] D. K. Singha, M. Ghosh, R. Majhi, and R. Mohanta, Optimal configuration of Protvino to ORCA experiment for hierarchy and non-standard interactions, J. High Energy Phys. 05 (2022) 117.
[46] B. Abi *et al.* (DUNE Collaboration), Experiment simulation configurations approximating DUNE TDR, arXiv:2103.04797.

[47] G. L. Fogli, E. Lisi, A. Marrone, D. Montanino, and A. Palazzo, Getting the most from the statistical analysis of solar neutrino oscillations, Phys. Rev. D **66**, 053010 (2002).

[48] P. Huber, M. Lindner, and W. Winter, Superbeams versus neutrino factories, Nucl. Phys. **B645**, 3 (2002).

[49] M. Dentler, A. Hernández-Cabezudo, J. Kopp, P. A. N. Machado, M. Maltoni, I. Martinez-Soler, and T. Schwetz, Updated global analysis of neutrino oscillations in the presence of eV-scale sterile neutrinos, J. High Energy Phys. 08 (2018) 010.

[50] C. Bronner, Recent results and future prospects from T2K, *Proceedings of the Neutrino 2022 Conference* (2022).

[51] J. Hartnell, New results from the NOνA experiment, *Proceedings of the Neutrino 2022 Conference* (2022).

[52] A. Donini, K.-i. Fuki, J. Lopez-Pavon, D. Meloni, and O. Yasuda, The discovery channel at the Neutrino Factory: $\nu(\mu) \to \nu(\tau)$ pointing to sterile neutrinos, J. High Energy Phys. 08 (2009) 041.